plained by incorporating nonlocal loss mechanisms.

VII. SUMMARY

In this paper we have introduced a simple model which is believed to describe the relevant influence of a boundary on the polariton waves. In contrast to the considerations in Ref. 2, we do not neglect the coupling to light in the boundary-condition problem. Generally, our treatment leads to the condition that an appropriate linear combination of P and $\partial P/\partial x$ vanishes at the surface [see Eq. (16)]. However, when inserting actual parameters of crystalline resonances we find that $P=0$ at the surface is an adequate condition throughout the spectrum. The influence of the thickness a of the surface layer has been treated strictly in the long-wave limit. Thus, if a polariton mode carrying a considerable part of the energy has a wave vector comparable to $1/a$, then a more elaborate calculation is necessary.[2] We have also extended the theory of bulk waves and boundary conditions to include two or more dispersive resonances. Finally, we have demonstrated the agreement with experiment of the boundary condition in case of the exciton lines in ZnO.

[1]S. I. Pekar, Zh. Eksperim. i Teor. Fiz. 33, 1022 (1957) [Sov. Phys. JETP 6, 785 (1958)].

[2]J. J. Hopfield and D. G. Thomas, Phys. Rev. 132, 563 (1963).

[3]J. J. Hopfield, J. Phys. Soc. Japan, Suppl. 21, 777 (1966).

[4]V. M. Agranovich and V. L. Ginzburg, *Spatial Dispersion in Crystal Optics and the Theory of Excitons* (Interscience, John Wiley and Sons, London, 1966).

[5]C. W. Deutsche and C. A. Mead, Phys. Rev. 158, A63 (1965).

[6]J. J. Hopfield, Phys. Rev. 112, 1555 (1958).

[7]D. G. Thomas, J. Phys. Chem. Solids 15, 86 (1960).

[8]Y. S. Park and J. R. Schneider, J. Appl. Phys. 39, 3049 (1968).

[9]J. Filinski and T. Skettrup (unpublished).

[10]M. Cardona, J. Phys. Chem. Solids 24, 1543 (1963) ($M=0.9m_0$).

[11]D. E. Dietz, J. J. Hopfield, and D. G. Thomas, J. Appl. Phys. 32 Suppl. 2282 (1961). ($M=1.5m_0$, if corrected for the new value of the electron mass, $m_e=0.25m_0$).

[12]B. Segall, Phys. Rev. 163, 769 (1967) ($M=2m_0$).

[13]The time-saving approximations introduced in previous computations of exciton spectra in ZnO (see Ref. 13) have not been applied here. Consequently, we obtain somewhat different values for oscillator strengths and resonance frequencies.

[14]T. Skettrup, Solid State Commun. 7, 869 (1969).

[15]T. Skettrup and I. Balslev, Phys. Stat. Solidi 40, 93 (1970).

PHYSICAL REVIEW B VOLUME 3, NUMBER 4 15 FEBRUARY 1971

Focusing of Phonons in Crystalline Solids due to Elastic Anisotropy*

B. Taylor, H. J. Maris, and C. Elbaum
Department of Physics, Brown University, Providence, Rhode Island 02912
(Received 14 September 1970)

Large differences (up to a factor of 100) have been observed in the intensity of phonons of different polarizations propagating ballistically in LiF, KCl, and Al_2O_3. These observations were made by means of heat-pulse experiments carried out on single crystals, in the temperature range 1.5–3.5 °K. The results are explained in terms of phonon focusing due to the fact that in elastically anisotropic crystals the phonon phase and group velocities are, in general, not collinear. Calculations of the focusing effect, to determine the relative intensities of phonons of each polarization in many crystal directions, have been carried out for a number of solids. The results of these calculations are in good agreement with the experimental results obtained in this study, as well as with those obtained by other investigators on Si, Ge, and NaF.

I. INTRODUCTION

In heat-pulse experiments,[1] phonons are generated in a thin metallic film on one face of a crystal by means of short electrical, microwave, or laser pulses. The phonons are detected, after propagating through the crystal, by means of a suitable bolometer. Metallic films which undergo a superconducting-to-normal transition when the phonon energy arrives are very effective detectors. For heat-pulse experiments, a crystal with phonon mean free path comparable to its linear dimensions is required so that the phonons will propagate ballistically rather than diffusively. Pulses due to phonons of different polarizations then arrive at the detector at different times and therefore can be studied independently. These experiments have considerable advantages over thermal-conductivity studies

as a means of investigating phonon-phonon and phonon-defect interactions. For example, the scattering of phonons by crystal defects may be studied by introducing the defects into the crystal and determining the fraction of phonons of a given polarization which travel unscattered from the generator to the detector. Heat-pulse studies thus make it possible to investigate the scattering of phonons of different polarization separately. This is in contrast to thermal-conductivity measurements, which only give some average scattering rate for all phonons. Another advantage of heat-pulse studies is that the propagation of groups of phonons with wave vectors lying in specified directions can be investigated, whereas, again, thermal conductivity involves a complicated average over $\vec{k}$ space.

In this paper we report experimental results on lithium fluoride, potassium chloride, and sapphire, which show that the heat pulses due to phonons of some polarizations may have much larger amplitudes than others. The ratio of the amplitudes of heat pulses of differing polarizations is often as much as a factor of 100, and for some of the crystals investigated pulses of certain polarizations are too small to be observed at all in certain directions. To ascertain whether this effect was due to preferential scattering of one type of phonon, experiments were performed on samples of different thicknesses. It was found that the ratio of the intensities of longitudinal and transverse phonons was approximately independent of the thickness, which indicated that no preferential scattering was occurring.

It has been proposed[2] that this effect (called here phonon focusing) is a consequence of elastic anisotropy. The phonons generated by the film are assumed to have an approximately uniform distribution of directions of wave vectors. However, because the wave vector and group velocity are not collinear, a uniform distribution of directions in $\vec{k}$ space does not lead to a uniform distribution of energy flux. The amount of energy (and hence the heat-pulse amplitude) received thus depends upon the crystallographic direction between the detector and the generator. The energy received varies for the different phonon polarizations since the deviation of the group-velocity direction from the wave-vector direction is different for each polarization.

Calculations to determine the relative intensities of phonons of each polarization in a number of directions have been carried out for LiF, Si, Ge, KCl, NaF, CaF_2, and Al_2O_3. The relative intensities calculated on the basis of the phonon-focusing effect are in good agreement with the results of heat-pulse experiments in all the solids studied, i.e., LiF, KCl, and Al_2O_3.

Large differences in the relative intensities of longitudinal and transverse phonons have also been previously observed in the $\langle 100 \rangle$ directions in silicon and germanium by Pomerantz and von Gutfeld.[3] A similar but smaller effect was observed in sodium fluoride by Rogers and Rollefson.[4] The explanation proposed here also accounts for these results.

II. CALCULATIONS

The object of these calculations is to determine (i) the angular relation between wave vectors and the corresponding group-velocity vectors, for all directions of phonon propagation; (ii) the energy flux along specified crystal directions resulting from a pulse of phonons having a uniform angular distribution of wave vectors.

A. Calculation of Group-Velocity Vectors

In the present investigation, the phase velocities and corresponding displacement vectors were determined, as a function of direction, using the known values of the second-order elastic constants. These results were then used to calculate the corresponding group velocity from the relationship of Miller and Musgrave[5] and from that of Fedorov.[6]

Musgrave used a variational technique to derive the following relationship for the components of the group velocity $\vec{v}$ in a cubic crystal:

$$V_\alpha = [l_\alpha^2 C_{44} + A_\alpha^2(\rho v^2 - C_{44})]/\rho v l_\alpha ,$$

where summation over repeated indices is not assumed, $\vec{l}$ is the unit vector in the direction of the phase velocity $\vec{v}$, $\vec{A}$ is the unit displacement vector, ρ is the density, and C_{44} is the conventional elastic constant.

Fedorov's expression is

$$V_\epsilon = C_{\alpha\epsilon\gamma\delta}\ l_\delta\ A_\alpha\ A_\gamma/\rho v ,$$

where summation over repeated Greek subscripts is implied and $C_{\alpha\epsilon\gamma\delta}$ are elastic constants.

Both expressions given above were used to compute the components of the group velocity, and the results obtained by the two methods were identical.

Cross sections of the group-velocity surfaces of lithium fluoride and potassium chloride in several planes have been plotted using the data thus computed; two examples are presented in Figs. 1 and 2 which show the cross sections in the (100) plane for lithium fluoride and potassium chloride, respectively.

B. Calculation of Energy Flux

1. *Statistical Method*

For crystals of cubic symmetry, a computer calculation was performed of the number of group-velocity vectors lying within each of a large number of small solid angles spanning the irreducible symmetry triangle for a uniform angular distribution of wave vectors. The values of the elastic constants used were those of Alers *et al.*[7] for lithium fluoride

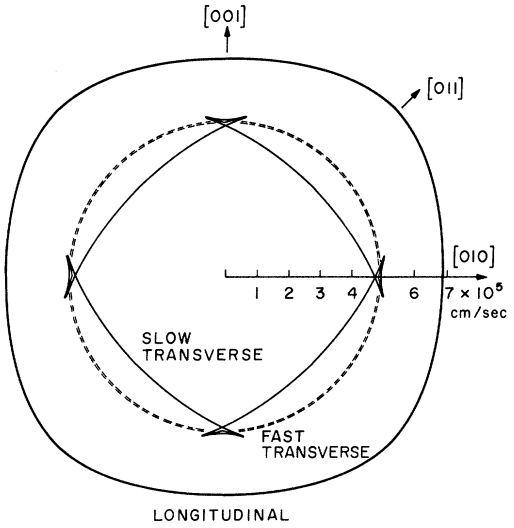

FIG. 1. Cross section of the group-velocity surfaces of lithium fluoride in a {100} plane.

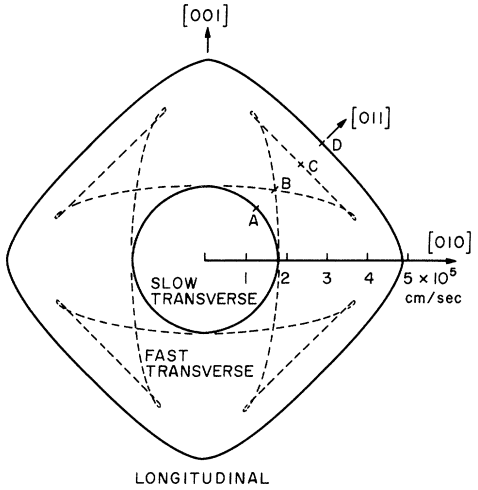

FIG. 2. Cross section of the group-velocity surfaces in potassium chloride in a {100} plane.

($C_{11}=1.246$, $C_{12}=0.424$, and $C_{44}=0.649$ in units of 10^{12} dyn/cm^2, density $\rho=2.646$ gm cm^{-3}, temperature = 0 °K) and those of Norwood *et al.*[8] for potassium chloride ($C_{11}=0.483$, $C_{12}=0.054$, and $C_{44}=0.066$, in the same units, $\rho=2.038$ gm cm^{-3}, temperature = 4 °K).

A conventional spherical coordinate system was used, with $\theta=0°$ representing the [001] direction, $\theta=90°$, $\phi=0°$ representing the [100] direction, and $\theta=90°$, $\phi=90°$ representing the [010] direction.

The directions of the wave vectors were made to range over the region $25° \leq \theta \leq 120°$, $-30° \leq \phi \leq 75°$ for the lithium-fluoride computation, and over the region $1° \leq \theta \leq 134°$, $-44° \leq \phi \leq 89°$ for potassium chloride. These regions were made to extend well beyond the [100]-[110]-[111] triangle, which was used as the standard region, to ensure that all group velocities lying *inside* and associated with wave vectors lying *outside* the triangle were included. The region was made larger for potassium chloride than for lithium fluoride as the maximum deviation between the wave vector and group velocity is larger for this crystal. Wave vectors were taken at $\frac{1}{2}°$ intervals in θ and ϕ throughout the selected regions, and the corresponding number of group-velocity vectors of each polarization was computed in "boxes" $2° \times 2°$. In the absence of focusing, i.e., for an isotropic solid, each box would thus contain 16 group-velocity vectors, that is, one such vector for each wave vector. A correction was applied to compensate for variations in the solid angles subtended at the origin by equal increments in θ and ϕ, for different values of θ.

Tables I – VI show the phonon densities for each of the three polarizations in lithium fluoride and potassium chloride. The coordinates specified in these tables are those of the centers of the mesh used in the computation. For clarity and conciseness, alternate rows and columns in the original tables have been omitted. Statistical fluctuations due to the small number of group-velocity vectors

TABLE I. Calculated densities for longitudinal phonons in lithium fluoride. Densities ≥ 1.0 are underlined.

θ° \ ϕ°	0	4	8	12	16	20	24	28	32	36	40	44
46	1.5	1.5	1.5	1.4	1.6	1.6	1.7	1.8	1.9	1.9	2.0	1.9
50	1.6	1.1	1.5	1.4	1.4	1.7	1.8	1.9	2.1	2.0	2.2	1.9
54	1.2	1.4	1.2	1.2	1.4	1.4	1.6	1.8	1.9	2.2	2.3	2.3
58	1.0	0.9	0.7	0.9	1.1	1.1	1.4	1.6	1.8	2.1	2.2	2.1
62	1.0	0.5	0.7	0.8	0.7	1.0	1.2	1.3	1.6	1.8	1.9	2.1
66	0.8	0.5	0.4	0.5	0.7	0.7	0.9	1.1	1.4	1.7	1.9	2.2
70	0.6	0.4	0.3	0.6	0.6	0.6	0.8	1.0	1.2	1.5	1.7	1.9
74	0.6	0.4	0.4	0.3	0.4	0.6	0.7	0.8	1.0	1.5	1.8	1.3
78	0.1	0.3	0.3	0.3	0.5	0.4	0.4	0.8	0.9	1.1	1.3	1.4
82	0.1	0.3	0.5	0.3	0.4	0.4	0.5	0.8	0.6	1.2	1.3	1.5
86	0.1	0.3	0.3	0.3	0.4	0.4	0.5	0.9	1.0	0.9	1.5	1.4
90	0.1	0.1	0.1	0.4	0.6	0.6	0.8	0.9	0.9	1.1	1.5	1.3

TABLE II. Calculated densities for fast-transverse phonons in lithium fluoride. Densities ≥1.0 are underlined.

θ° \ ϕ°	0	4	8	12	16	20	24	28	32	36	40	44
46	11.0	1.2	0.8	0.5	0.3	0.2	0.2	0.0	0.0	0.0	0.0	0.0
50	11.1	1.2	0.7	0.7	0.4	0.2	0.2	0.0	0.0	0.0	0.0	0.0
54	11.4	1.1	0.6	0.4	0.3	0.3	0.2	0.0	0.0	0.0	0.0	0.0
58	11.6	0.9	0.7	0.6	0.4	0.4	0.1	0.0	0.0	0.0	0.0	0.0
62	14.8	0.9	0.6	0.5	0.4	0.4	0.2	0.2	0.0	0.0	0.0	0.0
66	12.6	0.9	0.7	0.5	0.4	0.5	0.2	0.2	0.1	0.0	0.0	0.0
70	10.8	0.8	0.6	0.5	0.4	0.4	0.3	0.2	0.1	0.2	0.1	0.1
74	9.0	0.7	0.6	0.4	0.5	0.4	0.4	0.3	0.3	0.2	0.2	0.3
78	7.0	0.6	0.6	0.6	0.5	0.4	0.4	0.4	0.5	0.5	0.3	0.5
82	5.1	0.7	0.6	0.6	0.5	0.5	0.6	0.6	0.6	0.6	0.6	0.6
86	3.0	0.7	0.7	0.7	0.9	0.7	0.9	0.8	0.9	0.9	1.1	1.0
90	1.7	3.1	5.2	7.1	8.7	10.4	11.9	13.3	14.3	14.6	13.1	11.4

associated with each box were present, especially in regions of low density. In all cases, the results presented in the tables have been normalized so that the density would be unity for an isotropic medium.

2. *Analytic Method*

The phonon densities were also calculated by an analytic method developed by Maris.[9] In this method the phase velocities and displacement vectors calculated in the statistical program were used. The effects of small deviations of the direction of the wave vector on the directions of the corresponding group-velocity vectors were determined. For an elastically isotropic material, the deviations are the same, but for the anisotropic materials they are not, and the degree of focusing or defocusing is given by the ratio of the solid angles defined by two small perpendicular deviations in the wave vector and by the corresponding deviations in the group-velocity vector.[10] This ratio was computed for waves of each of the three polarizations at 2° intervals in the θ and ϕ coordinates of the wave vector in the region $45^\circ \leq \theta \leq 100^\circ$, $0^\circ \leq \phi \leq 60^\circ$. The correlation between the density factors obtained statistically and analytically was very satisfactory bearing in mind the statistical fluctuations mentioned previously. The largest discrepancies were observed near cusps where the density varies very rapidly with angle; the different results are obtained because the statistical method gives an average intensity over a finite solid angle, whereas the analytic method effectively considers an infinitesimal solid angle.

3. *Phonon Transmission Coefficients*

In this investigation it was assumed that (i) the relative abundance of phonons of the three possible polarizations generated is approximately the same in all experiments; (ii) the angular distribution of their wave vectors (momenta) is approximately constant over a range extending roughly 30° for LiF and 40° for KCl about the normal (propagation) direction, these angles being the maximum deviation between phase and group velocities in these two solids.

The same type of generator was used in all experiments. It is therefore considered reasonable to assume the above conditions, provided that there is not a strong dependence of the relative abundance of phonons of different polarizations or of the angular distribution of momenta on the nature of the gen-

TABLE III. Calculated densities for slow-transverse phonons in lithium fluoride. Densities ≥1.0 are underlined.

θ° \ ϕ°	0	4	8	12	16	20	24	28	32	36	40	44
46	0.2	0.4	0.3	0.1	0.3	0.2	0.2	0.2	0.1	0.2	2.0	1.9
50	0.4	0.3	0.3	0.3	0.1	0.2	0.2	0.3	0.3	0.5	2.3	2.9
54	0.5	0.3	0.3	0.3	0.1	0.2	0.3	0.3	0.3	1.5	2.7	2.2
58	0.3	0.3	0.3	0.2	0.2	0.3	0.3	0.4	1.9	1.6	3.2	2.4
62	0.3	0.3	0.3	0.2	0.3	0.3	1.2	1.3	0.9	1.5	1.8	0.5
66	0.3	0.3	0.2	0.3	0.3	2.0	1.2	1.0	1.9	0.2	0.2	0.3
70	0.3	0.4	0.4	0.3	2.1	1.3	1.2	1.8	0.2	0.1	0.2	0.3
74	0.3	0.3	0.8	1.7	1.4	1.3	1.4	0.2	0.3	0.4	0.3	0.2
78	0.3	1.9	1.8	1.4	1.5	1.2	0.2	0.4	0.4	0.3	0.3	0.3
82	13.3	1.8	1.6	1.6	1.2	0.3	0.2	0.4	0.3	0.3	0.4	0.3
86	13.0	10.5	1.7	2.2	0.4	0.4	0.3	0.3	0.4	0.4	0.4	0.3
90	8.7	13.3	13.4	0.4	0.4	0.4	0.4	0.4	0.4	0.4	0.4	0.4

TABLE IV. Calculated densities for longitudinal phonons in potassium chloride. Densities ≥ 1.0 are underlined.

θ° \ φ°	0	4	8	12	16	20	24	28	32	36	40	44
46	0.0	0.5	0.5	0.3	0.1	0.2	0.1	0.1	0.1	0.1	0.1	0.1
50	0.6	0.6	0.4	0.3	0.2	0.1	0.1	0.1	0.1	0.1	0.1	0.1
54	0.7	0.5	0.5	0.2	0.2	0.1	0.1	0.1	0.1	0.1	0.1	0.1
58	0.7	0.6	0.5	0.3	0.2	0.2	0.2	0.2	0.1	0.1	0.1	0.2
62	0.8	0.7	0.4	0.3	0.3	0.1	0.2	0.1	0.1	0.1	0.1	0.1
66	0.8	0.9	0.6	0.3	0.2	0.1	0.2	0.2	0.1	0.1	0.1	0.1
70	1.0	1.2	0.8	0.4	0.3	0.2	0.2	0.1	0.1	0.1	0.1	0.1
74	2.1	1.6	1.1	0.5	0.4	0.3	0.3	0.2	0.2	0.2	0.2	0.2
78	3.6	2.8	1.7	1.0	0.7	0.5	0.2	0.3	0.2	0.2	0.2	0.2
82	8.2	5.6	3.0	1.6	1.1	0.8	0.8	0.4	0.4	0.4	0.4	0.4
86	15.9	11.7	5.3	2.9	1.3	1.3	0.6	0.6	0.6	0.6	0.6	0.6
90	22.5	15.7	8.1	3.7	2.4	0.8	0.8	0.7	0.7	0.7	0.7	0.7

erator-sample boundary.

The calculation of the transmission coefficients is based on the approach of Little,[11] who determined the rate of phonon emission per unit area $P(T_1, T_0)$, where T_1 and T_0 are the temperatures of the generator and of the sample, respectively. On the assumption of an isotropic source and sample, Little obtained the following expression, which has a form similar to the Stephan-Boltzmann law for photon radiation:

$$P(T_1, T_0) = (\pi^5/15h^3)\,[\langle t\rangle_L^{(10)}/(v_L^{(1)})^2 + 2\langle t\rangle_T^{(10)}/(v_T^{(1)})^2]\, k_B^4\,(T_1^4 - T_0^4), \qquad (1)$$

where $v_L^{(1)}$ and $v_T^{(1)}$ are the velocities of the longitudinal and transverse phonons in the generator, and $\langle t\rangle_L^{(10)}$ and $\langle t\rangle_T^{(10)}$ are the corresponding phonon-transmission coefficients from generator to sample, averaged over all angles of incidence. The subscripts on the transmission coefficients indicate the phonon polarization in the generator. The transmitted phonon may have a different polarization.

The factors $(v_L^{(1)})^{-2}$ and $2(v_T^{(1)})^{-2}$ in Eq. (1) are proportional to the products of the densities of states times the velocities of longitudinal and (degenerate) transverse phonons in the generator. The ratio of longitudinal and transverse phonons incident on the generator-sample boundary is $\frac{1}{2}(v_T^{(1)}/v_L^{(1)})^2$.

The particular transmission coefficients which are of the greatest importance in the present investigation are those for the forward direction, denoted here by t_{ij}, where the i, j subscripts indicate the phonon polarizations in the generator and sample, respectively. These may be derived from the conditions that the normal and tangential displacements and stresses must be the same on both sides of the boundary between the generator and sample.[12]

For a boundary between two isotropic media, or normal to principal directions in anisotropic media, these transmission coefficients have the simple form[13]

$$t_{ij} = 0, \quad i \neq j \qquad (2)$$

$$t_{ii} = 4\rho^{(1)} v_i^{(1)} \rho^{(0)} v_i^{(0)}/(\rho^{(1)} v_i^{(1)} + \rho^{(0)} v_i^{(0)})^2, \qquad (3)$$

TABLE V. Calculated densities for fast-transverse phonons in potassium chloride. Densities ≥ 1.0 are underlined.

θ° \ φ°	0	4	8	12	16	18a	20	24	28	32	36	40	44
46	1.4	1.1	0.8	0.7	1.3	0.4	0.3	0.1	0.2	0.3	0.4	0.2	0.2
50	1.5	1.1	1.0	0.6	0.4	0.5	0.1	0.3	0.5	0.2	0.2	0.1	0.4
54	0.9	1.3	0.9	0.5	0.3	0.2	0.2	0.1	0.6	0.3	0.2	0.4	0.2
58	1.6	1.4	1.2	0.6	0.3	0.2	0.2	0.4	0.4	0.5	0.3	0.1	0.3
62	2.6	1.9	1.2	0.5	0.3	0.3	0.2	0.8	0.4	0.3	0.2	0.3	0.2
66	3.5	2.6	1.7	0.9	0.6	0.4	0.2	0.8	0.4	0.4	0.4	0.2	0.5
70	5.8	4.6	2.9	1.7	1.2	0.8	1.9	1.1	0.8	0.7	0.1	0.1	0.2
72[a]	10.4	9.3	6.9	2.4	0.8	0.5	0.9	0.4	0.2	0.3	0.1	0.2	0.0
74	6.6	4.6	0.0	0.0	0.1	0.1	1.5	0.5	0.4	0.2	0.1	0.3	0.3
78	0.0	0.0	0.0	0.0	0.0	1.6	1.7	0.7	0.5	0.5	0.3	0.4	0.6
82	0.1	0.0	0.1	0.0	0.0	5.9	2.7	1.4	1.1	0.9	0.8	0.9	0.3
86	0.1	0.1	0.0	0.0	3.6	9.9	4.9	2.8	1.5	1.2	1.1	1.2	0.6
90	0.1	0.2	0.1	0.0	6.4	10.6	6.0	3.4	2.7	1.4	1.3	1.3	0.9

[a]This row or column would normally be omitted as the table includes only alternate rows and columns. It has been included in this case as it contains very high values for the density.

TABLE VI. Calculated densities for slow-transverse phonons in potassium chloride. Densities ≥1.0 are underlined.

$\theta°$ \ $\phi°$	0	4	8	12	16	20	24	28	32	36	40	44
46	0.3	0.2	0.0	0.2	2.0	1.3	1.1	1.3	1.1	1.0	1.0	1.1
50	0.2	0.2	0.0	0.2	1.7	1.3	1.1	1.3	1.0	0.9	0.8	0.9
54	0.3	0.2	0.0	0.8	2.0	1.5	1.2	1.4	1.3	0.9	0.9	0.8
58	0.3	0.2	0.0	0.6	2.6	1.6	1.4	1.4	1.5	1.0	0.7	0.9
62	0.3	0.2	0.1	0.2	2.9	1.5	1.5	1.6	1.6	1.3	0.9	0.9
66	0.3	0.2	0.5	0.5	4.5	2.4	1.8	1.8	1.6	1.1	1.0	1.1
70	0.3	0.2	0.1	0.3	5.8	2.6	2.3	1.8	1.5	1.1	0.7	0.8
74	0.3	0.3	0.3	0.5	18.3	7.3	3.9	2.5	1.9	1.8	1.6	1.6
78	0.2	0.5	0.3	0.5	0.5	0.3	0.6	0.3	0.6	0.8	1.7	2.2
82	0.3	0.3	0.1	0.2	0.3	0.0	0.4	0.4	0.2	0.0	0.0	0.0
86	0.4	0.6	0.3	0.6	0.4	0.3	0.3	0.3	0.3	0.3	0.3	0.2
90	0.6	0.4	0.3	0.3	0.3	0.3	0.3	0.3	0.3	0.3	0.3	0.3

where $\rho^{(1)}$ and $\rho^{(0)}$ are the densities of the generator and sample, and $v_i^{(1)}$ and $v_i^{(0)}$ are the corresponding phase velocities for polarization i.

For principal directions of propagation, the calculated values of these transmission coefficients from constantan into lithium fluoride are in the range 0.81–0.93. For potassium chloride they range from 0.47–0.69, and for sapphire from 0.99–1.00. These transmission coefficients do not change the ratio of the intensities of phonons of different polarizations by more than 10% in lithium fluoride, 45% in potassium chloride, and 1% in sapphire.

The density of phonons propagating in a small solid angle about the forward direction is also affected by refraction at the generator-sample boundary. Phonons incident within a cone of semiangle $\theta_i^{(1)}$ about the normal will be refracted into a cone of semiangle $\theta_i^{(0)}$, where $\theta_i^{(1)}$ and $\theta_i^{(0)}$ are related to the phase velocities in the source and sample $v_i^{(1)}$ and $v_i^{(0)}$ by Snell's law:

$$\sin\theta_i^{(1)}/\sin\theta_i^{(0)} = v_i^{(1)}/v_i^{(0)} . \quad (4)$$

The flux of phonons about the forward direction will be changed by a factor of $(\theta_i^{(1)}/\theta_i^{(0)})^2$, which for small angles is approximately equal to $(\sin\theta_i^{(1)}/\sin\theta_i^{(0)})^2$ or $(v_i^{(1)}/v_i^{(0)})^2$.

Calculated values of $(v_i^{(1)}/v_i^{(0)})^2$ for the directions of propagation used in lithium fluoride, potassium chloride, and sapphire are in the ranges 0.27–0.57, 0.66–2.15, and 0.16–0.22, respectively. Refraction at the generator-sample boundary changes the ratio of the intensities of phonons of different polarizations by factors of up to 2.1 in lithium fluoride, 3.3 in potassium chloride, and 1.3 in sapphire.

As previously stated, pulses of phonons were detected by observing the increase produced by their arrival in the electrical resistance of a film of an indium-tin alloy. It is necessary, therefore, also to consider the phonon-transmission characteristics between the sample and the detector. For phonons incident in the normal direction to the indium-tin films, these coefficients may be obtained from Eqs. (2) and (3). Their values range from 0.89–1.00 for lithium fluoride, from 0.89–1.00 for potassium chloride, and from 0.63–0.84 for sapphire. These values were obtained using approximate average velocities of longitudinal and transverse phonons in indium (2.6×10^5 cm/sec and 0.9×10^5 cm/sec), calculated from the elastic constants of indium listed by Truell, Elbaum, and Chick.[14]

III. EXPERIMENTAL EQUIPMENT AND PROCEDURE

Single crystals of "ultraviolet-grade" lithium fluoride and of "optical-grade" potassium chloride, supplied by the Harshaw Chemical Company, were used. The single-crystal sapphire used was supplied by the "Industrie de Pierres Scientifiques," Monthey, Switzerland. The samples were mounted in high-conductivity copper holders, and located in an evacuated can immersed in liquid helium. Care was taken to maintain good thermal contact between the sample, its holder, and the helium bath. The phonon sources consisted of thin (1000–3000-Å) resistive films of constantan which were vapor deposited at a pressure below 10^{-5} Torr (typically 5×10^{-6} Torr). The thickness of the films was determined by weighing the mass of constantan deposited on an exposed area of a glass slide located next to the sample during the evaporation. It was also estimated from the mass of constantan evaporated, with good consistency between the two methods. Films of the required linear dimensions were obtained by the use of evaporation masks made of aluminum or stainless-steel foils. Electrical contact with the source films was established by means of films of silver evaporated at the extremities of the constantan. Contact with the silver was achieved using spring-loaded brass pins with indium-foil tips.

Phonons were generated by heating the constantan films with short (typically 10^{-7} sec) pulses of electric current. A repetition rate of 100 times per

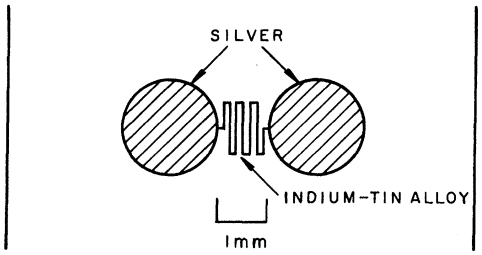

FIG. 3. Schematic diagram showing the convoluted shape of the indium-tin detector and the silver contacts.

sec was used. It was found that the repetition rate could be increased to 700–800 times per sec without producing a measurable increase in the ambient temperature for an input power level of about 10 W for the duration of the pulse.

In order to simplify the theoretical interpretation of the experimental results, it is advantageous that the source and detector define only a small solid angle of propagation directions. For this purpose it is necessary to use a source and detector of small linear dimensions. However, the temperature of the source, for a fixed power input, increases as the area of the source decreases. For this reason, sources of dimensions 1×1 and 2×2 mm were used for most of this investigation.

Phonons were detected by means of evaporated indium-tin–alloy films approximately 4000 Å in thickness. The alloy used for evaporation was 94% indium, 6% tin, but the deposited films had a reduced tin content due to the lower vapor pressure of this constituent. A tin-rich residue was left in the evaporation crucible. Evaporation was carried out under a pressure of less than 10^{-5} Torr and typically 5×10^{-6} Torr. The detectors were deposited in the form of narrow highly convoluted strips, as shown in Fig. 3, by the use of stainless-steel masks. The masks were prepared by coating 0.001-in.-thick stainless-steel foil with Kodak Metal Etch Resist, removing the protective resist in the desired region by a photographic process, and etching through the foil with a solution of 3 parts water, 1 part concentrated nitric acid, and 1 part concentrated hydrochloric acid. In this way, a detector of total length 7 mm and width 0.1 mm was produced in an area of 1×1 mm. The convoluted shape was used to obtain detectors of high resistance while keeping their over-all linear dimensions small.

Electrical contact with the detectors was made by the same method as used for the sources. The resistance of the detectors decreased by a factor of approximately 10 on cooling from room temperature to 4 °K. The detectors became superconducting at approximately 3.5 °K in the absence of an applied magnetic field, with a transitional range of about 100 mdeg. Over a certain portion of the superconducting-normal transition the resistance of the detector varied approximately linearly with the temperature, and it was in this region that measurements were made.

A magnetic field in the plane of the films was applied to lower the temperature of the superconducting-normal transition when measurements were made at temperatures below 3.5 °K. At these lower temperatures the temperature range of the transition increased to several hundred millidegrees.

A steady dc bias current of 5–10 mA was passed through the detector. A load resistance of 1000 Ω was connected in series with the detector, whose resistance was within the range of 0–50 Ω and was typically 1–10 Ω, to prevent large fluctuations in the detector current as its resistance varied.

Figure 4 is a block diagram of the electronic equipment used. The electrical pulses applied to the source were supplied by an E-H Research Laboratories 131-2 pulse generator which had a rise time of 20 nsec and a maximum power output of 50 W. The pulses were displayed on an oscilloscope, with a 25-MHz bandwidth, to facilitate measurement of the input voltage and pulsewidth.

The signals produced by the arrival of heat pulses were amplified 40 dB by means of a Hewlett-Packard 462A amplifier with a rise time of less than 4 nsec and overshoot of less than 5%. The amplified pulses were displayed on another channel of the oscilloscope described above. The amplifier had a maximum output of approximately 1.2 V. Detected pulses having amplitudes greater than 12 mV saturated the amplifier.

The dc bias voltage across the detector was displayed on the Y axis of an X-Y recorder. The position on the superconducting-normal transition of the detector could be monitored continuously in this way. A resistance of 10 kΩ was inserted in the line and a 0.01-μF capacitor to ground connected

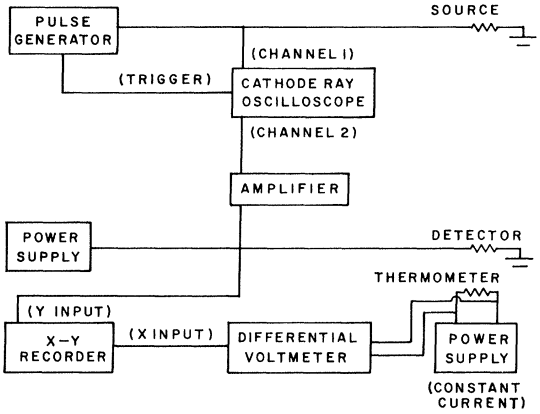

FIG. 4. Block diagram of the electronic equipment.

TABLE VII. Summary of experimental and calculated results.

Solid	Direction	Intensity ratio (Long: fast trans: slow trans) Expt	Calc (uncorr)	Calc (corr)	Velocities (10^5 cm/sec) Expt	Calc
Al_2O_3	X	2:8:1	5:9:1	1.5:6:1	11.1, 6.9 5.9	11.19, 6.81 5.82
Al_2O_3	Z[a]	1:1.5	...	...	11.4, 6.35	11.22, 6.15
LiF	[100][a]	1:100	1:60	1:120	6.8, 4.9	6.86, 4.95
LiF	[110]	2:20:1	5:25:1	1.5:16:1	7.3, 4.9 3.9	7.49, 4.95 3.94
LiF	[111][a]	1:2	1:1	1:3	7.3, 4.2	7.69, 4.30
KCl	[100][a]	15:1	55:1	9:1	4.8, 1.8	4.86, 1.80
KCl	[110]	1.5:1:3:1[b]	4:4:4:1	0.8:2:2:1	3.9, 3.2, 2.5, 1.8	4.05, 3.24 ~2.4, 1.80
KCl	[310] ($\theta=90°$, $\phi=18°$)	1:6:1[c]	25:100:1 :3.5	6.5:100:1 :5.5	4.5, 3.7 1.9	4.50, 3.85 1.87, 1.80
KCl	[311] ($\theta=72°$, $\phi=18°$)	1:30:5[d]	1:4:10: 0.05:1.5	1:15:40 :0.15:6	4.1, 3.4, 1.8	4.10, 3.45, 3.14 1.92 1.85

[a]Transverse modes degenerate.

[b]Two fast-transverse pulses-velocity-surface overlaps.

[c]Two fast-transverse pulses; second fast-transverse pulse (1.87×10^5 cm/sec) and slow-transverse pulse (1.80×10^5 cm/sec) not resolved.

[d]Two fast- and two slow-transverse pulses. First fast-transverse pulse (3.45×10^5 cm/sec) and first slow-transverse pulse (3.14×10^5 cm/sec) not resolved. Second fast-transverse pulse (1.92×10^5 cm/sec) and second slow-transverse pulse (1.85×10^5 cm/sec) not resolved. Pulses listed in order of velocities.

across the recorder input to prevent noise from the recorder entering the amplifier.

The temperature of the sample was measured by means of a carbon resistance thermometer mounted on the copper sample holder.

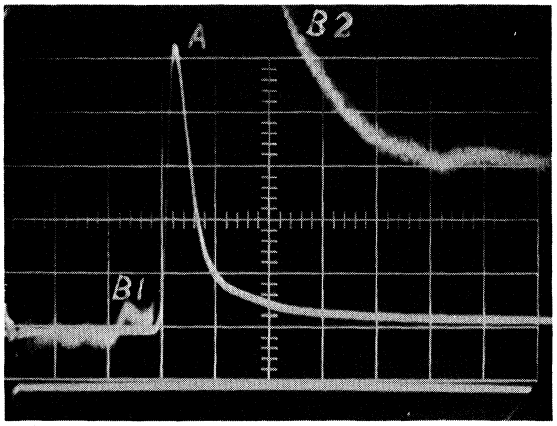

FIG. 5. Heat pulses in a ⟨100⟩ direction in lithium fluoride. Double exposure was used to obtain trace A with a vertical scale of 0.2 V/(major division) and traces B1 and B2 with a vertical scale of 0.02 V/(major division). The pulse B1 corresponds to longitudinal phonons and was not visible at the amplification of trace A. Time scale, 0.5 μsec/(major division); path length, 6.8 mm; temperature, 3.5 °K.

IV. RESULTS

Heat pulses were propagated in the ⟨100⟩, ⟨110⟩, and ⟨111⟩ directions in lithium fluoride, in the ⟨100⟩, ⟨110⟩, ⟨310⟩, and ⟨311⟩ directions in potassium chloride, and in the Z (threefold-symmetry) and X (twofold-symmetry) directions in sapphire. A summary of all experimental and calculated results is given in Table VII.

For propagation in all directions except the ⟨310⟩ and ⟨311⟩ directions, crystals with faces normal to the propagation direction were prepared. For propagation in the ⟨310⟩ and ⟨311⟩ directions, crystals with {100} faces were used, with the source and detector offset the required distance.

The path length used was typically about 1 cm for the lithium fluoride and potassium chloride, and was 2 cm for the sapphire.

In the ⟨100⟩ direction in lithium fluoride, the intensity of the (degenerate) transverse pulse exceeded that of the longitudinal pulse by a factor of approximately 100, as shown in Fig. 5. In contrast to this result, in the same direction in potassium chloride, the intensity of the longitudinal pulse exceeded that of the transverse pulse by a factor of approximately 15, as shown in Fig. 6.

In the ⟨110⟩ direction in lithium fluoride, the ra-

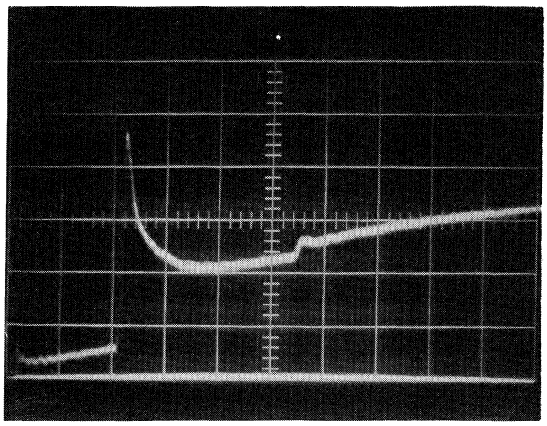

FIG. 6. Heat pulses in the ⟨100⟩ direction in potassium chloride. Vertical scale, 0.02 V/(major division); time scale, 1.0 μsec/(major division); path length, 9.9 mm; temperature, 3.1°K.

tio of the intensities of the longitudinal, fast-transverse, and slow-transverse pulses was approximately 2:20:1, as shown in Fig. 7. In the same direction in potassium chloride (Fig. 8), four pulses were observed having intensities in the ratio 1.5:1:3:1. These pulses are labeled A, B, C, and D and are associated, respectively, with the portions of the group-velocity surface shown in Fig. 2 and marked by the same letters. The extra pulse observed in potassium chloride occurs because of the large cusp in the transverse-group-velocity surface about the ⟨110⟩ direction.

Pulses were propagated in the ⟨310⟩ and ⟨311⟩ directions in potassium chloride because the calculation predicted high intensities for the fast-transverse mode in the ⟨310⟩ direction and for the slow-transverse mode in the ⟨311⟩ direction. These high intensities were associated with the edges of cusps on the group-velocity surfaces, and were in fact observed with transit times corresponding to their predicted velocities.

Two sets of calculated results are presented in Table VII. The first column gives the expected ratios of the various phonons present on the basis of the focusing effect alone. For the alkali halides the results of the statistical calculation were used, averaged over all the directions subtended by the source and detector. These results were weighted in favor of those directions associated with the largest areas of the source and detector. In the case of sapphire, a statistical calculation was not performed and the results of the analytic method are shown.[15]

The second column of calculated intensity ratios listed in Table VII was obtained from the first by multiplying by the following four ratios: (i) the ratio of the abundances of longitudinal and transverse phonons in the source. Assuming constantan to be isotropic, and using the values $v_L^{(1)} = 5.24 \times 10^5$ cm sec^{-1} and $v_T^{(1)} = 2.64 \times 10^5$ cm sec^{-1} reported by Weis[13] this ratio is approximately 1:4:4, with the degeneracy of the transverse phonons having been disregarded; (ii) the ratio of the transmission coefficients from source to sample $t_{LL}:t_{TT}:t_{SS}$, where L, T, and S signify longitudinal, fast-transverse and slow-transverse phonons; (iii) the ratio of the refraction factors $(v_L^{(1)}/v_L^{(0)})^2:(v_T^{(1)}/v_T^{(0)})^2:(v_S^{(1)}/v_S^{(0)})^2$; (iv) the ratio of the transmission coefficients from sample to detector $t_{LL}:t_{TT}:t_{SS}$. In calculating the intensity ratios in the ⟨310⟩ and ⟨311⟩ directions, the transmission coefficients for the ⟨100⟩ direction were used.

As seen in Table VII for all materials and directions investigated experimentally, the ratio of the intensities of the pulses observed was in good qualitative agreement with the ratio predicted theoretically, especially after the corrections described above had been applied. It was not possible to compare intensities of pulses observed in different directions because of variations in the characteristics of the generators and detectors used.

The experimental and calculated velocities of the pulses studied are also listed in Table VII. The experimental velocities were taken as the path length divided by the time between the beginning of the input pulse and the onset of the detected pulse. The accuracy of the experimental values for the phonon velocities is estimated to be about ±5%. The principal source of error was in locating the onset of the detected pulse, especially in cases of low intensity and of superimposed pulses. The discrepancies between the observed and predicted phonon velocities were within the estimated limit of error in all cases.

In order to investigate the possibility of selective scattering of phonons of a particular polarization,

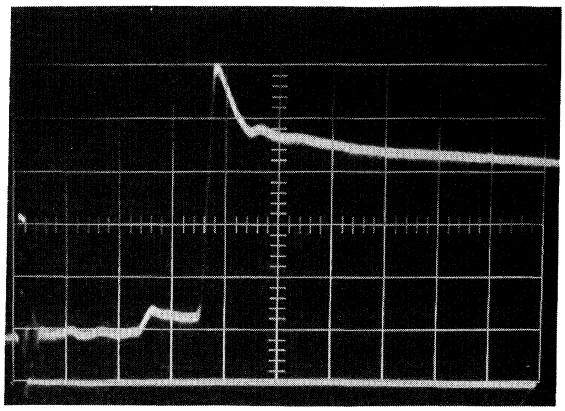

FIG. 7. Heat pulses in the ⟨110⟩ direction in lithium fluoride. Vertical scale 0.05 V/(major division); time scale, 0.5 μsec/(major division); path length, 8.4 mm; temperature, 1.4°K.

experiments were carried out on samples of different path lengths. Phonon propagation in the ⟨100⟩ direction in lithium fluoride and potassium chloride, and in the Z direction in sapphire was studied. It was found that the ratios of the intensities of phonons of different polarizations did not depend significantly on the path length. The path lengths used were 0.4–1.0 cm for the alkali halides studied and 1.4 and 2.0 cm for the sapphire.

V. DISCUSSION OF RESULTS

The experimental results have been explained in terms of a focusing mechanism dependent on the elastic anisotropy of the crystals. The correlation obtained between the experimental results and calculations based on the proposed explanation is very close. Furthermore, as mentioned previously, the ratio of the intensities of phonons of different polarizations did not depend appreciably on the path length. Selective scattering is not, therefore, the cause of the observed intensity ratios.

It is clear from a comparison of the experimental results and theoretical predictions listed in Table VII that there is a very close qualitative correlation between the two, especially when corrections have been applied for differences in the number of phonons generated and transmitted across the generator-sample and sample-detector boundaries, and for refraction effects. In all cases studied, with the exception of propagation in the ⟨110⟩ direction in potassium chloride, the order in terms of magnitude of the experimentally observed pulses was the same as the order predicted theoretically. In the case of propagation in the ⟨110⟩ direction in potassium chloride, both the predicted and observed intensity ratios were small, and the absolute magnitudes of the pulses were small, making an accurate comparison difficult. A difference in the predicted and observed order is of little significance under these conditions.

In general, the observed and predicted intensity ratios differed by not more than a factor of 2 or 3. This discrepancy is small in comparison with the ratios themselves, which were frequently in excess of 10:1. The mechanism by which the phonons were generated is not known with certainty. The estimated value of the relative abundance of longitudinal and transverse phonons entering the sample may therefore be inaccurate. There are also uncertainties in the transmission coefficients, as these were calculated for normal incidence, and the focusing effect depends on phonons which propagate in directions slightly inclined to the normal direction. Similar uncertainties are present in the calculations of the effects of refraction, as the approximation $\sin\theta \simeq \theta$ (for small values of θ) was used, and also because of variations in the phase velocities over the range of directions involved.

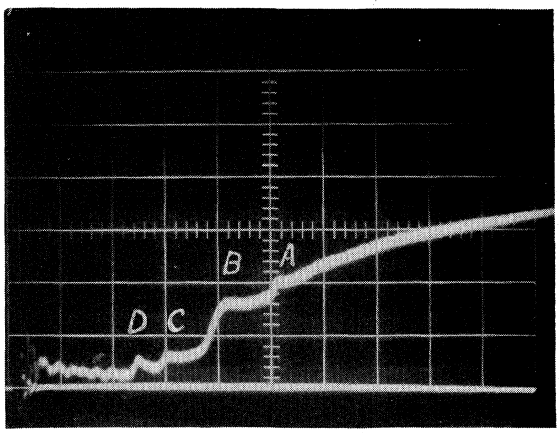

FIG. 8. Heat pulses in the ⟨110⟩ direction in potassium chloride. The pulses labeled A, B, C, D are associated, respectively, with the portions of the group-velocity surfaces shown in Fig. 2 and marked by the same letters. Vertical scale, 0.05 V/(major division); time scale, 1.0 μsec/(major division); path length, 9.0 mm; temperature, 3.0 °K.

There may be additional errors caused by deviations from linearity in the variation of the resistance of the detector with temperature, in the measurement of the pulse amplitudes, and in the use of these amplitudes as measures of the phonon intensities.

To calculate the degree of focusing of phonons in a cubic crystal, it is necessary to know only the three elastic constants C_{11}, C_{12}, and C_{44}. In fact, since the deviation between the group and phase velocities does not depend on the magnitudes of the elastic constants, but on their ratio, it is sufficient to know only $C_{11}:C_{12}:C_{44}$. For lithium fluoride this ratio is 1:0.34:0.52, and for silicon and germanium the ratios are 1:0.39:0.48 and 1:0.38:0.52. These three materials are therefore expected to have similar phonon-focusing properties, and observations made by Pomerantz *et al.*[3] on silicon and germanium, and on lithium fluoride in the present investigation, confirm that this is indeed the the case. For potassium chloride the ratio is 1:0.11:0.14 which differs considerably from those of the other three materials, as do the ratios of the longitudinal- and transverse-phonon intensities propagating along a given direction. Sodium fluoride has a ratio of elastic constants of 1:0.21:0.27; its phonon-focusing properties, as deduced from the observations of Rogers *et al.*,[4] are different from either of the two cases mentioned above and are in good agreement with the results calculated for this solid in the present study.

It is particularly noteworthy that lithium fluoride on the one hand, and silicon and germanium on the other, which differ drastically in most other prop-

erties, have similar phonon-focusing characteristics. The latter are directly relatable to the similarity in the ratios of their elastic constants, as mentioned above. This fact constitutes particularly strong evidence, in addition to the experimental evidence from the other alkali halides, for the validity of the focusing theory presented.

In view of these considerations, it is concluded that the correlation between the intensities of the pulses observed experimentally and those predicted theoretically from the elastic constants of the materials studied is sufficiently high to confirm the basic correctness of the theory used and the validity of the various assumptions made.

*Research supported in part by the National Science Foundation and by the Advanced Research Projects Agency.

[1]R. J. von Gutfeld, *Physical Acoustics* (Academic, New York, 1968), Vol. 5, p. 223.

[2]B. Taylor, H. J. Maris, and C. Elbaum, Phys. Rev. Letters 23, 416 (1969).

[3]M. Pomerantz and R. J. von Gutfeld, in *Proceedings of the Ninth International Conference on the Physics of Semiconductors*, edited by S. M. Ryvkin (Nauka Publishing House, Leningrad, 1968), Vol. 2, p. 690.

[4]S. J. Rogers and R. J. Rollefson, Bull. Am. Phys. Soc. 12, 339 (1967).

[5]G. F. Miller and M. J. P. Musgrave, Proc. Roy. Soc. (London) A236, 352 (1956).

[6]F. I. Fedorov, *Theory of Elastic Waves in Crystals* (Plenum, New York, 1968), p. 126.

[7]G. A. Alers and J. R. Neighbours, Rev. Mod. Phys. 31, 675 (1959).

[8]M. H. Norwood and C. V. Briscoe, Phys. Rev. 112, 45 (1958).

[9]H. J. Maris, J. Acoust. Soc. Am. (to be published).

[10]These deviations in the group-velocity vector are not necessarily mutually perpendicular.

[11]W. A. Little, Can. J. Phys. 37, 334 (1959).

[12]H. Kolsky, *Stress Waves in Solids* (Dover, New York, 1963), p. 31.

[13]O. Weis, Z. Angew. Phys. 26, 325 (1969).

[14]R. Truell, C. Elbaum, and B. B. Chick, *Ultrasonic Methods in Solid State Physics* (Academic, New York, 1969), p. 373.

[15]The values of the elastic constants of sapphire were taken from J. B. Wachtman, Jr., W. E. Tefft, D. G. Lam, and R. P. Stinchfield, J. Res. Natl. Bur. Std. (U. S.) 64A, 213 (1960).

PHYSICAL REVIEW B VOLUME 3, NUMBER 4 15 FEBRUARY 1971

Theory of Paraelectric Resonance and Relaxation

Leonard M. Sander*
University of Michigan, Ann Arbor, Michigan 48104
and
Herbert B. Shore†
University of California, San Diego, La Jolla, California 92037

(Received 16 July 1970)

The theory of paraelectric resonance (PER) and relaxation is reformulated to allow a consistent treatment of dynamic lattice processes, even in the case when coupling to the lattice is strong. A simple model Hamiltonian is used and certain response functions are calculated without using perturbation theory. It is shown that the main effect of the strong lattice coupling at low temperatures is to induce a renormalization of the tunneling parameter of the paraelectric dipoles. The structure of phonon sidebands in PER is discussed. The theory predicts a strong transfer of intensity from the PER lines to the sidebands above a certain characteristic temperature. A treatment is given of paraelectric relaxation using the same techniques. A calculation of the temperature dependence of dipole-lattice relaxation time agrees well with experiment with adjustment of two parameters.

I. INTRODUCTION

There has been a good deal of recent interest in "paraelectric" impurities in solids; that is, impurities which have electric dipole moments and rotational degrees of freedom.[1,2] The microwave spectroscopy of such impurities has come to be known as "paraelectric resonance" (PER).[3] In a PER experiment, an external electric field is applied to a sample containing paraelectric impurities, and the absorption of microwave radiation of fixed frequency is observed as a function of applied electric field. The analogy with paramagnetic resonance is obvious.

The best-known examples of PER are the experiments performed on substitutional OH^- impurities in a KCl host lattice. In this case, the OH^- aligns preferentially along the $\langle 100 \rangle$ axes of the host. Microwave-induced 90° tunneling transitions have been observed by several groups.[3]

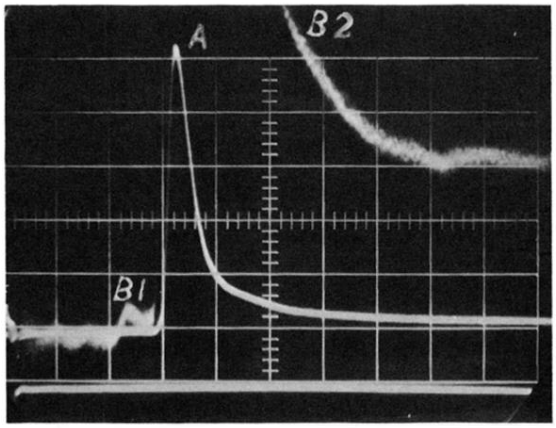

FIG. 5. Heat pulses in a ⟨100⟩ direction in lithium fluoride. Double exposure was used to obtain trace A with a vertical scale of 0.2 V/(major division) and traces B1 and B2 with a vertical scale of 0.02 V/(major division). The pulse B1 corresponds to longitudinal phonons and was not visible at the amplification of trace A. Time scale, 0.5 μsec/(major division); path length, 6.8 mm; temperature, 3.5 °K.

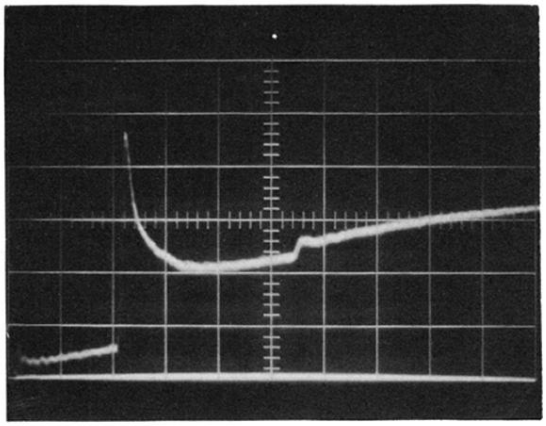

FIG. 6. Heat pulses in the ⟨100⟩ direction in potassium chloride. Vertical scale, 0.02 V/(major division); time scale, 1.0 μsec/(major division); path length, 9.9 mm; temperature, 3.1°K.

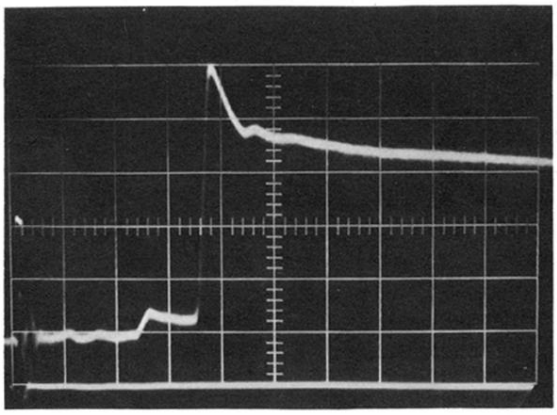

FIG. 7. Heat pulses in the ⟨110⟩ direction in lithium fluoride. Vertical scale 0.05 V/(major division); time scale, 0.5 μsec/(major division); path length, 8.4 mm; temperature, 1.4°K.

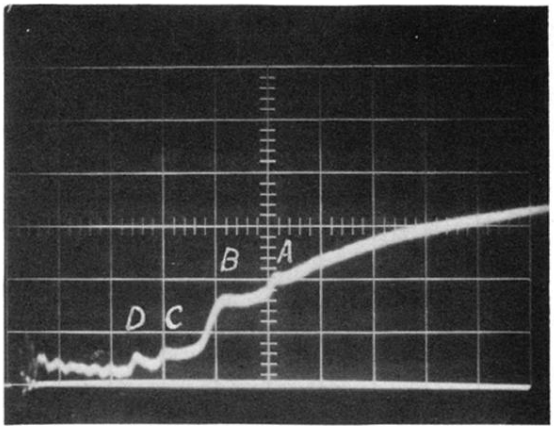

FIG. 8. Heat pulses in the ⟨110⟩ direction in potassium chloride. The pulses labeled A, B, C, D are associated, respectively, with the portions of the group-velocity surfaces shown in Fig. 2 and marked by the same letters. Vertical scale, 0.05 V/(major division); time scale, 1.0 μsec/(major division); path length, 9.0 mm; temperature, 3.0 °K.